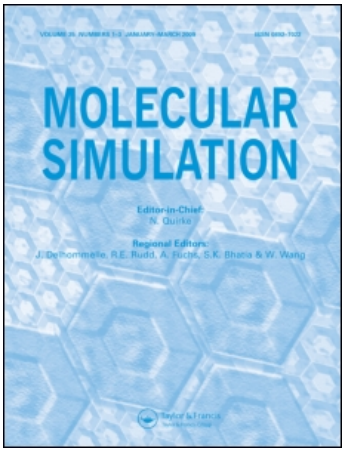

Molecular Simulation
Publication details, including instructions for authors and subscription information:
http://www.informaworld.com/smpp/title~content=t713644482

Molecular Mechanical Investigation of the Energetics of Butene Sorbed in H-Ferrierite

Fabien Jousse[a]; Laurence Leherte[a]; Daniel P. Vercauteren[a]
[a] Institute for Studies in Surface Science, Laboratoire de Physico-Chimie Informatique, Facultés Universitaires Notre-Dame de la Paix, Namur, Belgium

To cite this Article Jousse, Fabien , Leherte, Laurence and Vercauteren, Daniel P.(1996) 'Molecular Mechanical Investigation of the Energetics of Butene Sorbed in H-Ferrierite', Molecular Simulation, 17: 3, 175 — 196
To link to this Article: DOI: 10.1080/08927029608024106
URL: http://dx.doi.org/10.1080/08927029608024106

Molecular Simulation, 1996, Vol. 17, pp. 175–196
Reprints available directly from the publisher
Photocopying permitted by license only

MOLECULAR MECHANICAL INVESTIGATION OF THE ENERGETICS OF BUTENE SORBED IN H-FERRIERITE

FABIEN JOUSSE, LAURENCE LEHERTE and DANIEL P. VERCAUTEREN

Institute for Studies in Surface Science, Laboratoire de Physico-Chimie Informatique, Facultés Universitaires Notre-Dame de la Paix, rue de Bruxelles 61, B-5000 Namur Belgium

(*Received January 1996, accepted February 1996*)

The energetics and diffusion of the four butene isomers in a model of protonated ferrierite with Si/Al ratio of 8 is investigated using molecular mechanics, molecular dynamics, and a simple activated jump diffusion model, in order to determine the influence of the diffusion of the sorbent molecules onto the selectivity of ferrierite toward isobutene. Two main classes of adsorption sites are found, in the main 10-T channels and in cavities along 8-T channels. The magnitude of the self-diffusion coefficient mainly depends on the motions of the molecules in the 10-T channels, and it is found that isobutene diffuses more slowly than the linear isomers: at 623 K, D (isobutene) $< 0.03 \times 10^{-4}$ cm^2/s, while D (trans-2-butene) $\approx 0.42 \times 10^{-4}$ cm^2/s. However, the sites in the 8-T cavities act as molecular traps for linear butenes and slow down their diffusion, while they do not influence the self-diffusion of isobutene. Therefore, the diffusion of isobutene is enhanced relative to the other isomers in ferrierite, as compared with other zeolites with only one type of channels. This might be a reason for the good selectivity of ferrierite toward isobutene.

KEY WORDS: Butene isomerization, H-ferrierite, diffusion.

1 INTRODUCTION

Ferrierite has been shown recently to be a good catalyst for the skeletal isomerization of linear butenes to isobutene [1 – 4]; this reaction is commercially important, as isobutene is a precursor of MTBE, a high-octane gasoline additive. The excellent selectivity of ferrierite has been analysed to come from two factors [3]: its medium void space and medium acidity, which prevent the formation of oligomers but allow skeletal isomerization. Ferrierite (FER) is a natural and synthetic zeolite with orthorombic unit cell ($19.2 \times 14.1 \times 7.5$ Å)[5]. Its Si/Al ratio varies between 3.5 [5] and infinity [6]; most samples used for catalytic purposes exhibit a Si/Al ratio around 8 – 10 [7,8]. Its pore system consists of two intersecting channels, a 10-membered ring (10-T) channel along the z direction and a 8-membered ring (8-T) along y.

Though basic reasons for the high selectivity of FER are well established, it is still not completely understood why it is more selective than other zeolites showing similar topological and acidic properties, like ZSM-22 [9] or ZSM-23 [7]: these zeolites have an unidirectional 10-T ring channel system, and thus even less void space than ferrierite. So far, it has been supposed that the diffusion properties of butene molecuels in the channels of FER could explain this behavior [4].

Supposing that framework protons are randomly distributed on the bridging oxygens in FER, Xu *et al.* [3] found a close match between the pore volume accessible to the isobutene and 1-butene molecules (31 and 74%, respectively), and the percentage of protons located in the 10-T ring channels and in both 8- and 10-T ring channels (32 and 72%, respectively). These experimental results led the authors to conclude that 1-butene can enter the 8-ring channels while isobutene, due to its larger diameter cannot. Note that this conclusion is different from molecular dynamics simulations performed in a similar type of molecular sieve, the aluminophosphate DAF-1, where it was found that even linear butenes could not pass by the 8-T rings [10].

The aim of this study is to investigate the self-diffusion of butene in H-ferrierite, with the help of molecular mechanics techniques. The work has been divided in three parts: in a first step, we have investigated the location of aluminum atoms and bridging hydroxyl groups in a protonated ferrierite catalyst, in order to build a realistic model; a second part was devoted to the calculation of the energetics of the four isomers of butene, namely, 1-butene, trans-2-butene, cis-2-butene, and isobutene, sorbed in FER, in order to determine their self-diffusion. In a third Section, we present a simple model of activated jump diffusion, which was used to determine the influence of the topology of ferrierite on the diffusion of the butene isomers.

2 LOCATION OF THE HYDROXYL GROUPS

The substitution of silicon by aluminum in ferrierite has already been studied quantum-mechanically by Fripiat *et al.* [11]; it has been found to preferentially take place at a T1 site. However, this study did not take into account the hydroxyl group, which is likely to influence the energy of the configuration. Furthermore, the calculation was performed on a relatively small cluster (34 atoms at most), without taking into account the infinity of the crystal, and without geometry optimization. Calculations which include these effects may indeed lead to rather different resutls, as has been shown more recently by Schröder *et al.* [12], in the case of H-ZSM5. We have therefore studied the location of the Al sites and bridging hydroxyl groups in H-ferrierite, with the help of molecular mechanics (MM). We used the "czeo" variant of the cff91 forcefield, implemented in Biosym Technologies Discover package [13]. This forcefield, primarily designed to represent the interactions within and between organic molecules, takes explicitly into account the zeolitic hydroxyl groups. The parameters of the forcefield for these groups are based on *ab initio* calculations by Hill and Sauer [14]. Its computational form includes terms between bonded atoms as well as van der Waals and coulombic interactions. The charges placed on zeolitic ions derive from population analyses carried out at the *ab initio* level on model molecules. The charges actually used in the MM calculation are computed with help of bond increments δ_{ij} that represent the environment of each atom i: $q_i = \Sigma_j \delta_{ij}$, where j stands for each directly bonded atom. Table 1 lists the bond increments and van der Waals parameters for butene and ferrierite; parameters for bond interactions can be found in quoted documentation. Van der Waals energy is calculated as $E = \varepsilon_{ij}[2(r^*_{ij}/r_{ij})^9 - 3(r^*_{ij}/r_{ij})^6]$, with $r^*_{ij} = [r_i^6 + r_j^6]^{1/6}$ and $\varepsilon_{ij} = 2\sqrt{\varepsilon_i \varepsilon_j} r_i^3 r_j^3 / r_i^6 + r_j^6$. A cutoff at 9.5 Å was used for the van der Waals interactions; coulombic energy was

Table 1 Bond increments and van der Waals parameters for non-bonded interactions used for ferrierite and butene, from the forcefield cff91-czeo of Biosym Technologies [13, 14].

Bond increments		*van der Waals parameters*		
Bond	δ_i	*Element*	r_i(Å)	ε_i(*kcal/mol*)
oss[a]-Si	−0.1309	oss[a]	3.4506	0.1622
oas[b]-Si	−0.1265	oas[b]	5.2591	0.0129
oas[b]-Al	−0.1694	ob[c]	5.2191	0.0135
ob[c]-Si	−0.1392	Si	0	0
ob[c]-Al	−0.0284	Al	0	0
ob[c]-hb[d]	−0.0839	hb[d]	1.2149	5.2302
C—C	0	C—	4.01	0.054
C=C	0	C=	4.01	0.064
C—H	0.0530	H	2.9950	0.02

[a] Bridging oxygen linked to two Si ions
[b] Bridging oxygen linked to one Si and one Al
[c] Bridging oxygen linked to one Si, one Al, and one H
[d] Hydrogen in a bridging hydroxyl group

computed by Ewald summation. This forcefield has been used recently to study Al substitution in H-ZSM5 [15].

Ferrierite has four crystallographically different T sites and eight bridging oxygens, thus leading to twelve different locations for the Al ion and hydroxyl group (Fig. 1). Four of the oxygens are located at the crossing between the 8- and 10-T rings (O1, O6, O7, and O8), three at the crossing between the 6- and 8-T rings (O2,

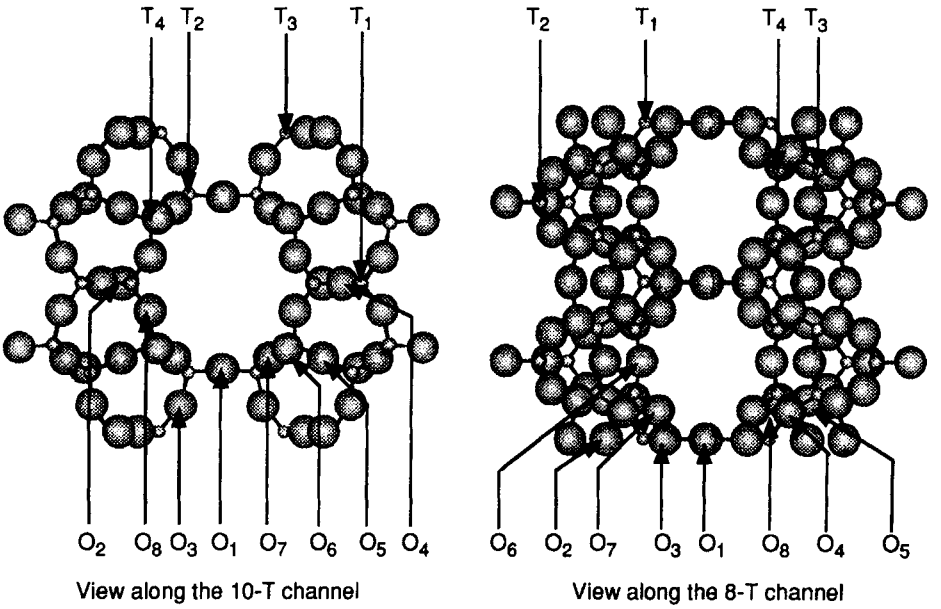

Figure 1 Position and numbering of the oxygen and tetrahedral atoms in purely siliceous ferrierite.

O3, O4), and one is part of the 5-T rings (O5). The influence of Al substitution is best viewed by considering a single T site in the calculation; however, the Si/Al ratio of H-ferrierite is usually quite low. Therefore we performed two series of simulations: in the first series, we considered the substitution of a single T-site in a simulation box consisting of two unit cells under periodic boundary conditions, that is, equivalent to a Si/Al ratio of 71; in the second series, four Al were substituted in the same crystallographic T site per unit cell of zeolite, thus giving a Si/Al ratio of 8. In the latter case, Löwenstein's rule determines univocally the position of each Al ion relative to the others. The first simulations give substitution energies, while the second show the influence of the distribution of the Al-OH groups in the crystal.

Table 2 gives the substitution energies for each site in the two models. The (T2, O7) site is favored in both cases, as the substitution energy for this site is lower by 16.7 kJ/mol (case 1) or 23.8 kJ/mol (case 2) with respect to the second lowest site. However, the substitution energies of 9 of the 12 sites lie within 40 kJ/mol of each other. A detailed analysis of the bonding, van der Waals, and electrostatic parts of the interaction shows that the ranking of the substitution energies is mainly due to van der Waals and bonding terms, while the electrostatic interaction energy values are very close to each other, and do not influence the ranking of the energies at all. Thus the substitution mainly takes place on steric and deformation criteria. This is also evidenced by the position of the proton, which is preferentially linked to an oxygen at the crossing of the 10-T ring and 8-T ring channels.

As can be seen from Table 2, the influence of the Si/Al ratio is small: for 8 of the 12 sites (Al on T3, for all H; H linked to O5, O7, and O8, for all Al substitution; Al on T2 with H linked to O3), the difference in the substitution energy between the two models is less than 4 kJ/mol. As for the other sites, a detailed energy analysis shows that the difference is due to the cumulative smaller differences between

Table 2 Substitution energy of a Si—O group by an Al—O—H group in H-ferrierite, as a function of the location of the substitution site. Calculations in case 1 are achieved using two unit cells and a single substitution, and in case 2 with one unit cell and four substitutions. The energy for case Si/Al = 8 has been divided by 4 to represent a single substitution. Figure 1 gives the labelling of the T and O sites. All energies are in kJ/mol.

	Case 1: Si/Al = 71				*Case 2: Si/Al = 8*
Site	*Total substitution energy*	*Van der Waals energy*	*Electrostatic energy*	*Internal energy*	*Total substitution energy*
T2, O7	−651.8	+16.1	−64.1	−603.8	−655.5
T2, O1	−611.0	+25.0	−58.2	−577.8	−617.9
T2, O3	−612.6	+18.3	−69.2	−561.7	−614.9
T1, O3	−594.6	+28.6	−68.8	−554.4	−584.9
T1, O4	−619.5	+26.4	−62.8	−582.6	−611.7
T4, O7	−619.9	+26.6	−65.4	−581.1	−618.3
T4, O8	−625.9	+28.5	−59.6	−594.8	−629.8
T4, O6	−626.8	+29.2	−72.7	−583.3	−613.3
T4, O5	−603.4	+31.1	−60.1	−573.4	−600.5
T3, O8	−635.0	+29.4	−65.4	−599.0	−631.9
T3, O2	−570.1	+31.9	−63.2	−538.8	−568.8
T3, O4	−623.4	+26.3	−57.8	−591.9	−624.1

bonding, van der Waals, and electrostatic energies. These differences appear in all case, but fortuitly cancel partially in the eight aforementioned sites.

Fripiat *et al.*, using an hexamere type model, have located the preferred substitution site on a T1 tetrahedron. This site was favored by 12 kJ/mol by comparison with the substitution on the T2 tetrahedron, while the sitting of an Al on a T3 or T4 site was found to be destabilized by more than 200 kJ/mol. When the calculations were performed with a monomeric or pentameric cluster, the substitution of an Al at a T2 site was favored. It was concluded, as both T1 and T2 sites lie in a 8-T ring, that substitution occurred preferentially on these rings.

Our results are somewhat different, as the preferred substitution site is found on a T2 tetrahedron with the proton linked to an O7 oxygen. The second preferred substitution site is found on a T3 tetrahedron, with the proton linked to an O8; here the influence of the proton is most apparent, as the substitution on a T3 site with the proton linked to an O2 oxygen is the less stabilized complex. Although the substitution energies remain rather close to each other for most sites, the three lowest energies correspond to protons lying in the 10-rings channels. This suggests that the repartition of the protons on the 10-rings channels is slightly favored.

3 ENERGETICS OF BUTENE IN H-FERRIERITE

This part of the work is devoted to the determination of the energetics of butene sorbent molecules in H-FER, in order to get informations on the self-diffusion of the various isomers in its porous system. The aforementioned studies of Xu *et al.* [3,4] indeed showed that diffusion of butene molecules in ferrierite is of great interest to understand the high selectivity toward isobutene in this zeolite. As most experimental measurements were performed with a zeolite with a Si/Al ratio close to 8, the model used here is the optimized structure which has been determined in the previous Section with the same Si/Al ratio: four protons per unit cell are linked to the O7 oxygens at the crossing between the 8- and 10-T ring channel systems, the aluminum being located on a T2 site. The same forcefield as in the previous Section was used. As it does not include any term for dipolar or polarization interactions, these were accounted for by placing charges on the atoms of both zeolite host and sorbent molecules. The butene charges were defined in the same way as for the zeolite (Tab. 1). Coulombic interactions were computed using a cutoff at 9.5 Å, which gives energy values very similar to the one computed using the Ewald summation method for this particular case, but with less computational effort. The consistency of the electrostatic energy values obtained by these two methods was verified on single point calculations in several conformations. The study has been divided in two parts. We first looked at the static interaction energies of butene isomers with H-ferrierite, by docking each isomer into the porous structure, then we investigated self-diffusion by molecular dynamics (MD) runs.

Only very few experimental data give interaction energies for molecules sorbed in H-ferrierite. In order to test the validity of the forcefield on this system, we performed preliminary molecular dynamics run on a related system, which has been extensively studied both theoretically and experimentally, namely, methane in silicalite [16]. The

same parameters as in Table 1 were used. At 300 K, the calculated adsorption energy of −15.9 kJ/mol is in reasonable agreement with available experimental data (−20.1 to −28.0 kJ/mol) [17], and with results obtained with other forcefields (−15.0 to −31.8 kJ/mol).

3.1 Docking

The minimum energy position of the four isomers of butene inside FER have been investigated using the docking procedure of Freeman *et al.* [18]. For each butene molecule, 100 initial configurations were generated from a high temperature (1000 K) MD run, and randomly set inside the zeolite structure, with an energy acceptance criterion that prevents any overlap of the molecule atoms with zeolite ones. The position and internal coordinates of the sorbent as well as of the zeolite structure were then optimized. This procedure locates numerous local energy minima, which could be roughly arranged in two classes: the global minimum is always located near the center of the cavity formed by the crossing between the 8- and 10-T ring channels, and an energetically close minimum, $\Delta E = 2 - 7.5$ kJ/mol, located inside the cavities of the 8-T ring channels. In Table 3 are listed the interaction energies associated with the deepest minima in each of those two classes, as well as the mean interaction energy calculated over the 100 minimized configurations. The position of the butene isomers corresponding to the two minima of Table 3 are depicted in Figure 2.

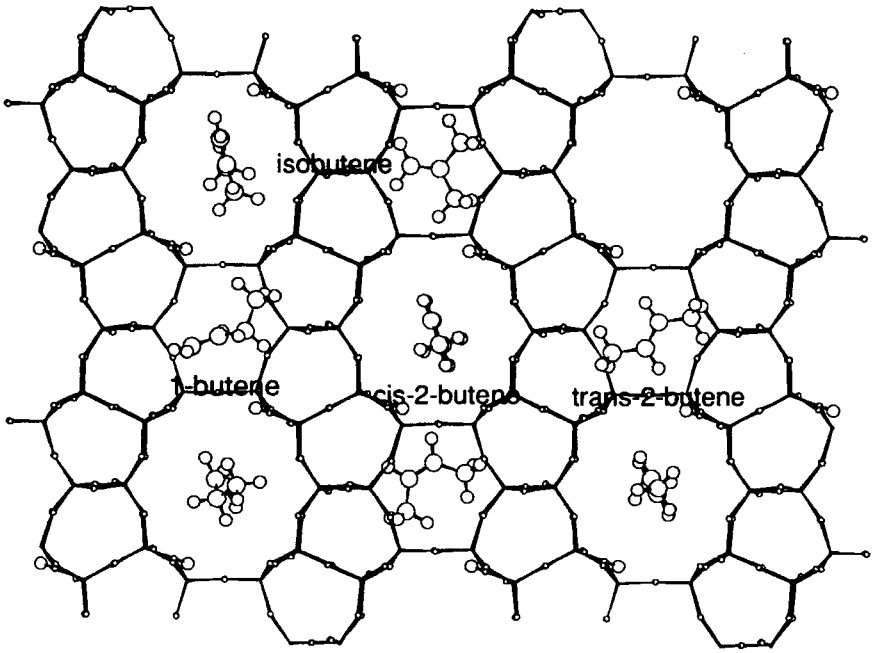

Figure 2 Minimum energy positions of the butene isomers in the 10-T ring channels (corresponding to the global energy minima) and in the 8-T ring cavities, computed with the docking strategy of Freeman *et al.* [18], with the cff91-czeo forcefield of Biosym.

Table 3 Interaction energy values (kJ/mol) of butene isomers within H-ferrierite, computed with the docking strategy of Freeman *et al.* [18], using the cff91-czeo forcefield of Biosym.

	1-butene	*trans-2-butene*	*cis-2-butene*	*isobutene*
global minimum	−38.83	−38.08	−35.85	−34.03
8-ring cavity minimum	−31.63	−30.57	−33.97	−27.71
mean energy over 100 dockings	−27.42	−25.00	−22.44	−25.49

We see, from Table 3, that isobutene is the less strongly adsorbed of all four isomers in the main channel system of ferrierite, as well as in the cavities along the 8-T channels. However, the differences are rather small: 4.8 kJ/ mol and 6.3 kJ/mol at the most in the 10- and 8-T ring channels, respectively. The mean energy over the 100 minimized configurations show a different ranking of the interaction energies, as isobutene seems more strongly sorbed than cis-or trans-2-butene.

As noted earlier, the energy minima in the 8-T ring cavities are energetically close to the values found in the larger channels. Thus, these sites appear to be *a priori* energetically accessible to all isomers. In all cases, the interaction energy in these 8-T sites is lower than the mean energy over the 100 minimized configurations, which again shows the high energetic stability of these minima.

3.2 *Molecular Dynamics*

Molecular dynamics (MD) is a very useful tool to investigate the mobility of molecules. Numerous MD studies have been devoted to simulate diffusion inside a zeolite structure [19]: through the analysis of the mean square displacement (MSD) of the center of mass with time, one can evaluate the diffusion coefficient D of the sorbent molecules inside the structure, using Einstein's relation [20]:

$$D = \lim_{t\to\infty} \frac{1}{6t} \int_0^\infty d\tau \, |\mathbf{r}(t+\tau) - \mathbf{r}(\tau)|^2 \tag{1}$$

However, one is limited by the length of the MD runs. Practically, this imposes a limit on the size of the sorbent molecules in a given zeolite as compared to the pore size, although some techniques (*e.g.* bias Monte-Carlo) now exist that allow the study of the energetics of hydrocarbon chains up to 40 atoms [21,22]. The velocity autocorrelation functions (VACF) of the center of mass of the sorbed molecules were also computed, in order to be used in the jump diffusion approach (*cf. Section 4*).

In the case of butene sorbed in ferrierite, long simulation runs are necessary in order to compute reliable diffusion properties. June *et al.* [23], and Hernández and Catlow [24] performed 500 and 1000 ps simulations, respectively, for butane in silicalite, a system comparable to ours. However, this is at the expense of the realism of the interaction model, which consisted in their work of van der Waals terms without any electrostatic interaction. The protons protruding from the framework in H-ferrierite is likely to create an electric field in the channel, which will influence the mobility of polar molecules like cis-2-butene or isobutene. The influence of these electrostatic

interactions has been rarely taken into account. Therefore, we chose to perform simulations with the same model as used for the docking study, and to limit the size of the system as well as the duration of the runs.

For each butene isomer, the dynamics of five molecules was studied using periodic boundary conditions in a simulation box consisting of four unit cells of the same optimized model of protonated ferrierite used in the docking study; the simulation box dimensions were $19.28 \times 28.80 \times 15.17$ Å. The zeolite atoms were held fixed during the simulations. Initial velocities of the atoms were attributed randomly according to a Boltzmann distribution at 623 K, which corresponds to the experimental conditions for butene isomerization [2, 3]. A 50 ps equilibration run was first performed in the constant number of particles, constant volume, constant temperature (NVT) ensemble, with a 1 fs time step, in order to reach an equilibrium at the desired temperature. Data were then collected during a 200 ps run in the microcanonical ensemble (NVE) with the same time step. From these data, the MSD of the center of mass of the butene isomers were computed, as well as thermodynamical averages. One run needs about 63 hours on an IBM RS/6000 model 560 computer with 128 Mb memory.

In order to evaluate the influence of the electrostatic interactions on the self-diffusion behavior of the sorbed butene molecuels, we also performed a 300 ps MD run in the same conditions but without considering coulombic interactions.

As we are mainly interested in the mobility of butene isomers in the 8-T ring channels, two initial positions were selected for each isomer: the position corresponding to the global energy minimum, as found in Section 3.1, and the local minimum energy position inside the 8-T cavity. During the simulation, molecules initially in the 10-T ring channels did not enter the 8-T cavities; similarly, molecules in the 8-T cavities could not step out. Consequently, the time-dependant MSD of the molecules initially in the 8-T cavities is simply a constant, close to zero. The time-dependant MSD of the butene isomers initially located in the 10-T channels are displayed in Figure 3. Due to the channel system of ferrierite, the MSDs are highly anisotropic, and only the displacement of the molecuels along the z axis contributes to the total MSD presented here. We also observe that there is no significative difference between the MSDs computed with and without electrostatic interactions. This clearly shows that the coulombic interactions have little influence on the diffusion of butene isomers in the channel system of protonated H-ferrierite. Table 4 sums up the computed diffusion coefficients. The MSDs reflect the steric forces between the guest molecules and the host structure, as D(trans-2-butene) > D(1-butene) $\approx$ D(cis-2-butene) > D(isobutene). During the simulation, isobutene could not step out of the main cavity; hence, the upper bound for its self-diffusion coefficient should be 0.03×10^{-4} cm^2/s. It appears from these qualitative results, that diffusion of isobutene in ferrierite is more hindered than that of all other isomers. However, other long-time effects may appear, invisible at this short time scale, that might modify our conclusions.

4 ACTIVATED JUMP DIFFUSION MODEL

The short length of the molecular dynamics simulations presented in the preceding Section prevents the observation of any diffusional behavior that would take place on

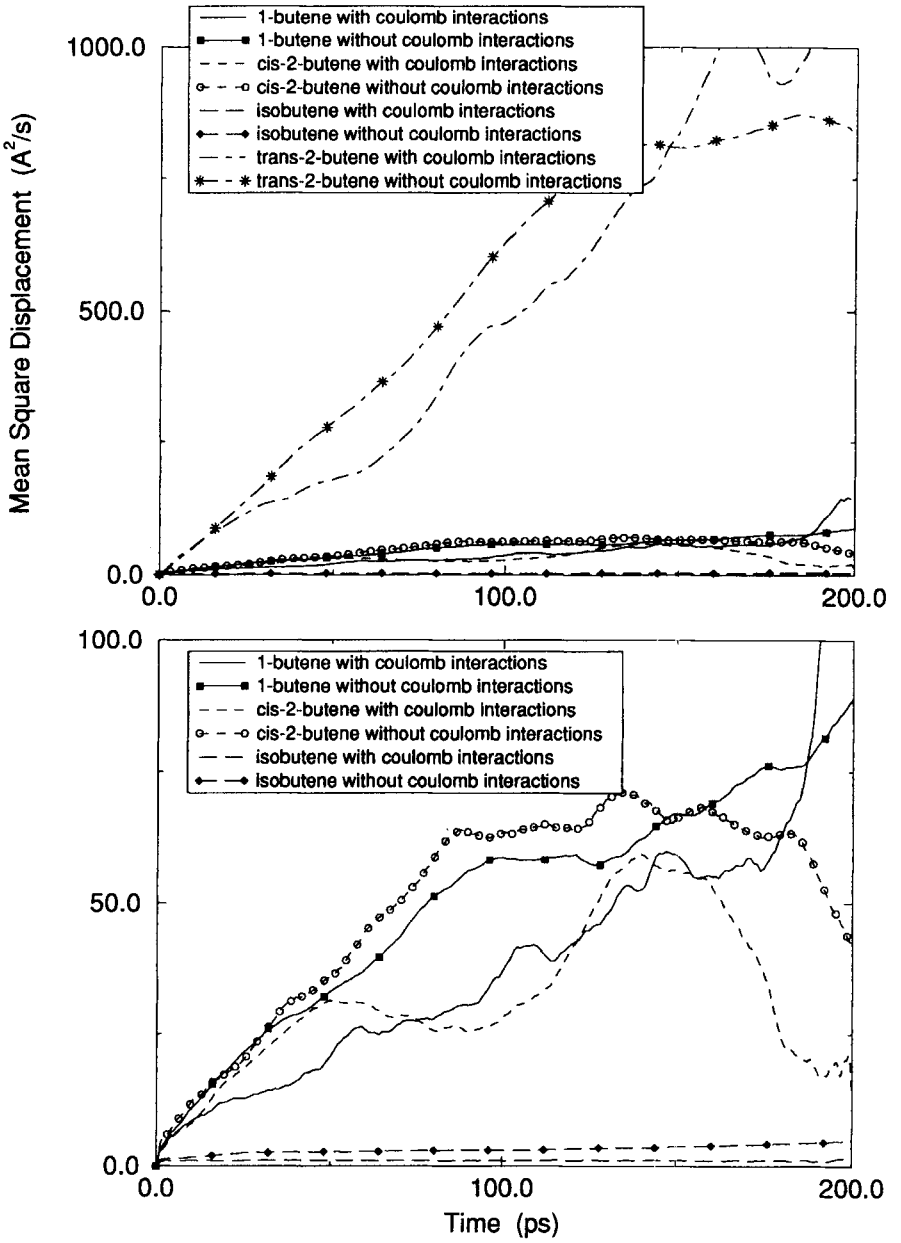

Figure 3 Mean square displacement of the four butene isomers in H-ferrierite, computed by a 200 ps molecular dynamics run at 623 K using Discover version 94.0 and the forcefield cff91-czeo of Biosym.

a longer time scale. In particular, as the molecules could not enter the 8-T cavities from the 10-T channels, the influence of the former sites could not be investigated. As mentioned in the Introduction, the possibility to enter these cavities seems however an important parameter in the selectivity toward isobutene in ferrierite. Indeed,

Table 4 Self-diffusion coefficient $D(10^{-4}\,cm^2/s)$ of butene isomers in H-ferriertite, computed from the result of a 200 ps molecular dynamics simulation at 623 K with the cff9-czeo forcefield of Biosym, and from the analytical solution of the jump diffusion model.

Diffusion Coefficient	*1-butene*	*trans-2-butene*	*cis-2-butene*	*isobutene*
From MD study	0.04	0.42	0.04	< 0.03
D_2 from Eq. 10(2 types of sites)	1.03	31.2	3.2	0.13
D_1 from Eq. 12(only sites 1)	1.5	32.0	3.7	0.18
From computation with JDM	1.03	31.2	3.2	0.18

Henson *et al.* [25] have shown by molecular dynamics simulations that the diffusion coefficient of sorbed xenon atoms is extremely dependant on the tortuosity of the channels of the zeolite. Hence, we have used a simple jump diffusion model (JMD) [26,27] in order to take into account the influence of both classes of energy minima on the diffusion. We emphasize that this hopping model is not intended to provide any quantitative results but to give informations on the diffusional behavior of the four butene isomers in ferrierite, and mainly on the influence of the minimum energy sites located in the 8-T cavities. We believe however that its simplicity itself is useful to understand this behavior.

4.1 Hopping Model

We have adopted the simplest model which keeps the main features of the butene + ferrierite system, namely, only two types of sites are considered, the first one corresponding to the main class of energy minima (the deepest one) located at the intersection between the 8-T and 10-T channels, while the second one represents the energy minima in the cavities along the 8-T channels. From a site 1 a molecule may hop to another site 1 along the z-axis with a rate constant k_{11}, or to a site 2 along y with a rate constant k_{12}; from a site 2 it can only hop to a site 1 with a rate constant k_{21}. This representation, sketched in Figure 4, does not accurately reflect the possible reorientation of the butene molecule in the zeolite channels, and thus is but a poor approximation to the real system. Nevertheless, we shall see its usefulness to understand the influence of the second site onto the diffusion.

A simple Arrhenius expression is assumed for the rate constants [28]:

$$k_{ij} = v_{ij}\exp(E_{ij}/kT) \tag{2}$$

E_{ij} is the activation energy to hop from site i to site j, and the basics for its calculation are given in the next paragraph. v_{ij} is a characteristic frequency of this motion. We believe that such an Arrhenius form of the rate constant is able to give a good view on the diffusional behavior, as very recently shown by Auerbach *et al.* [29] for the diffusion of benzene in Na-Y. A rigorous expression should be computed using Transition State Theory [30] or dynamically corrected TST [31]; however the many degrees of freedom of the system then would prevent any simple expression for the diffusion of the sorbed molecules. Therefore, we estimated the prefactor from the velocity autocorrelation functions (VACF) of the center of mass of the sorbent

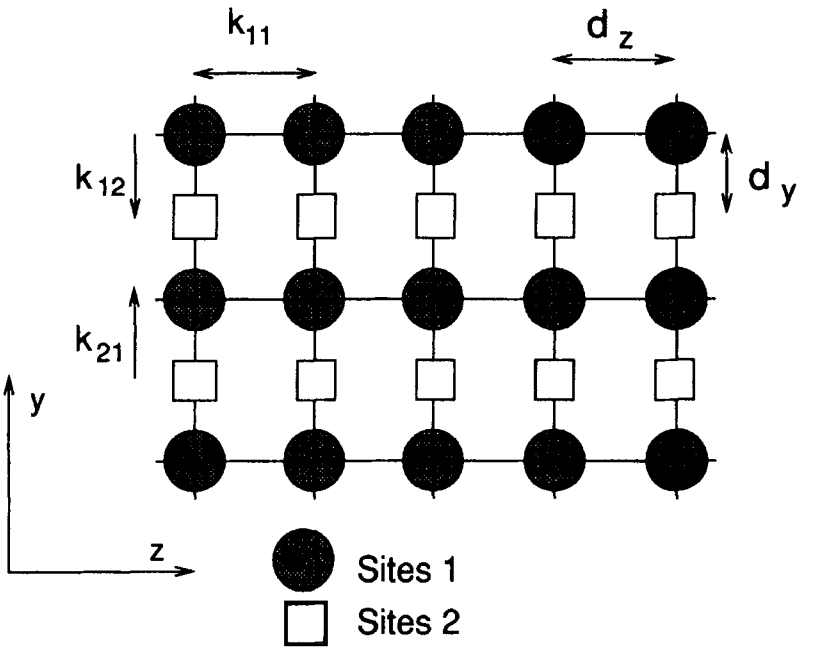

Figure 4 Model of jump-like diffusion for butene in ferrierite, considering only two types of interconnected sites.

molecules, as computed in Section 3.2. The Fourier Transform (FT) of the VACF gives indeed the typical frequencies of the system. Thus, an analysis of the VACF of the center of mass of the sorbed molecule along a specified direction should lead to acceptable estimations of the v_{ij}. More precisely, we shall make a correspondence between the FT of the VACF calculated in the 10-T channels along z, which is the direction of the motion from a site 1 to another site 1, and v_{11}; a similar correspondence is made between the FT of the VACF in the 10-T channels along y and v_{12}, and in the 8-T cavities along y and v_{21}.

The activation energies E_{ij} for the diffusion between sites i and j may be evaluated from the minimum energy pathway between the two minima corresponding to sites i and j. In order to determine these pathways, the molecule was moved step by step from its minimum position in site i to its minimum position in site j. At each step, one of the atoms of the molecule is constrained in a given plane perpendicular to the direction of the motion, with a quadratic force of the type $\omega^2(\alpha - \alpha_0)$, where α_0 is the coordinate of the plane. The whole structure, namely, the zeolite atoms, the other atoms of the molecule, and the two other degrees of freedom of the restrained atom, was then relaxed. This insures that the molecule may explore all of the energy surface during the stepwise motion in order to find the minimum energy pathway. After minimisation is achieved, the molecule is shifted in the given direction and α_0 is updated to the new position of the restrained atom.

Practically, the molecule was moved by 0.1 Å steps, starting from its minimum position in site 1 along z to another site 1, and along y to a site 2. The restrained force

has been set to 2090 kJ/mol. Å^2 (larger values led to the same energetic results). A 1000 fs molecular dynamics run was performed at each step before minimisation, as it was found that this leads to a smoother trajectory of the molecule. The potential energy along the minimum energy pathway "site 1 to site 1" and "site 1 to site 2" for all four butene isomers are shown in Figures 5a and b, respectively. The forces exerted by the framework on the displacement of the molecules decrease the effective length of the steps, so that, for example, up to ninety 0.1 Å steps are needed in order to move trans-2-butene from a site 1 to a site 2.

The activation energy along z is quite low for the butene isomers: 2 – 12 kJ/mol for linear butenes, and $\approx$ 30 kJ/mol for isobutene, to be compared with $kT = 5.18$ kJ/mol at 623 K. This shows that, especially for trans-2-butene, the description of the diffusion by activated jumps is inadequate. On the other hand, the potential energy barrier to the crossing of the 8-membered rings is high: from 67 kJ/mol for trans-2-butene to 200 kJ/mol for isobutene. This barrier has the same order of magnitude for linear butenes, while it is more than twice as high for isobutene. This suggests that the influence of the sites in the cavities along the 8-T channels might be very different for linear butenes and isobutene.

Table 5 sums up the activation energies E_{ij} determined from the calculation of the minimum energy pathway, as well as the frequenceis v_{ij}. From these values, we shall determine an order of magnitude of the diffusion coefficient of the butene isomers in ferrierite.

4.2 *Diffusion Coefficient from an Analytical Solution*

The random-walk problem for a molecule proceeding along a single axis by hops of length l and duration τ leads to the well-known expression of the diffusion coefficient [32]: $D = l^2/2\tau$. Similarly, the diffusion coefficient in our highly anisotropic system is best described by the relation:

$$D = \frac{1}{3}[D_y + D_z] = \frac{1}{6}\left[\frac{l_y^2}{\langle\tau_y\rangle} + \frac{l_z^2}{\langle\tau_z\rangle}\right] \tag{3}$$

$\langle\tau_y\rangle$ ($\langle\tau_z\rangle$, respectively) is the mean duration for a hop along y (z, respectively), independently of the number of jumps along z (y, respectively). These quantities can be obtained from the mean residence time in the sites 1 and 2, τ_1 and τ_2:

$$\tau_1 = \frac{1}{2(k_{11} + k_{12})}, \quad \text{and} \quad \tau_2 = \frac{1}{2k_{21}} \tag{4}$$

Let p be the probability of finding a molecule in a site 1, $p' = 1 - p$ its probability to be in a site 2; then, for a total of N jumps, the total duration is:

$$t = Np\tau_1 + N(1-p)\tau_2 \tag{5}$$

As the molecule is found $N(1-p)$ times in a site 2, it has jumped $N_y = 2 \times N(1-p)$

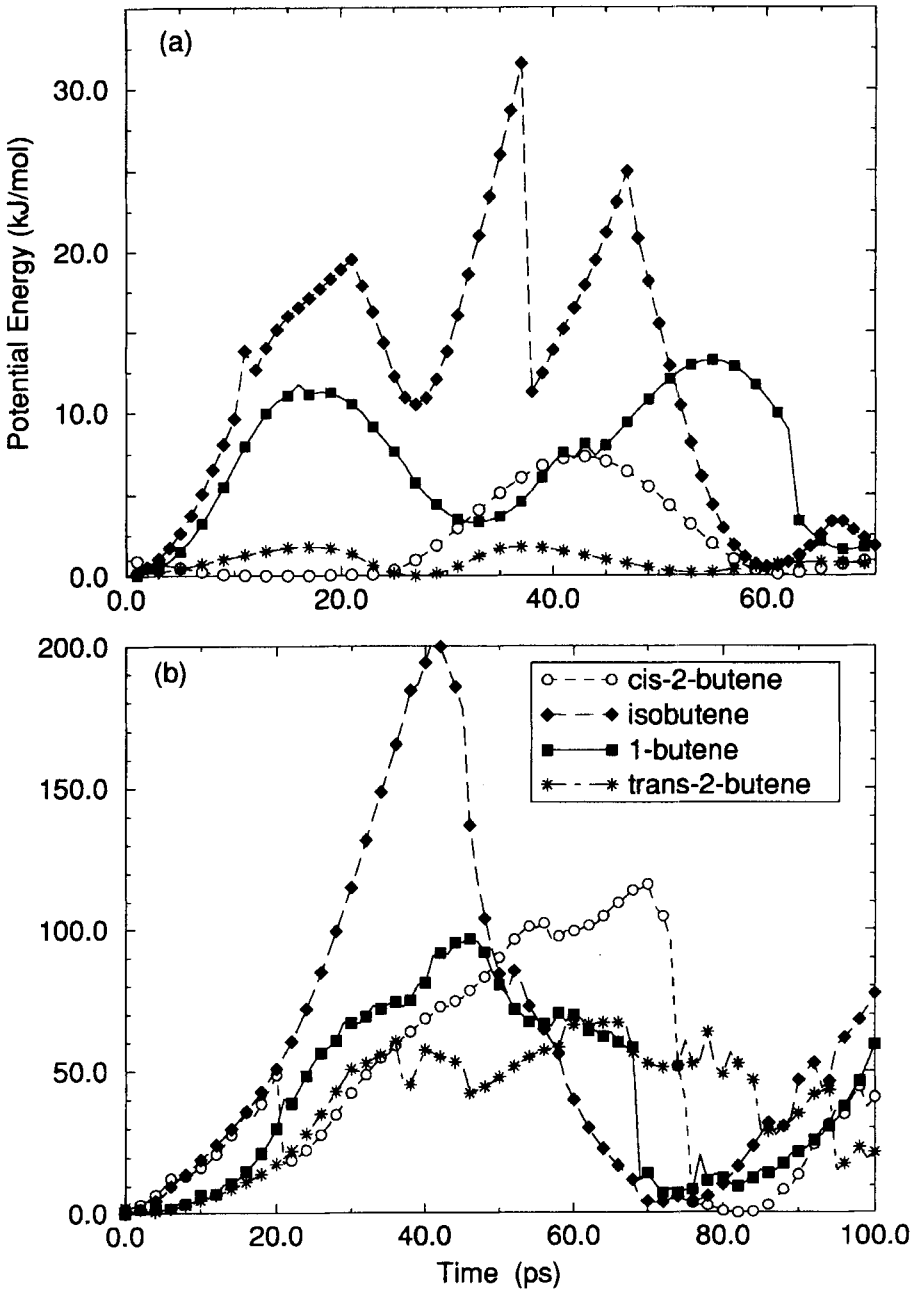

Figure 5 Minimum energy pathway from the minimum position of the molecule at the center of the cavity resulting from the crossing the 8- and 10-T channels, to (a) the same type of site and (b) the sites located in the cavity along the 8-T channels, determined from a constrained optimization of the molecule and zeolite structure at each 0.1 Å from site to site, using the cff91-czeo forcefield of Biosym.

Table 5 Activation energies E_{ij} and frequencies v_{ij} for butene isomers in ferrierite. The E_{ij} were determined by constrained optimization of molecule and zeolite along the minimum energy pathway from site i to site j; v_{ij} are estimated from the Fourier Transform of the Velocity Autocorrelation function of the center of mass of the sorbed isomers during a 200 ps molecular dynamics simulation at 623 K with the cff91-czeo forcefield of Biosym.

Molecule	E_{11} *(kJ/mol)*	$v_{11}(s^{-1})$	E_{12}	v_{12}	E_{21}	v_{21}
1-butene	12.0	0.8×10^{12}	97	2.0×10^{12}	90	2.0×10^{12}
trans-2-butene	2.1	2.5×10^{12}	67	3.0×10^{12}	60	2.5×10^{12}
cis-2-butene	8.4	1.0×10^{12}	113	3.0×10^{12}	111	2.5×10^{12}
iso-butene	30.0	1.2×10^{12}	200	2.0×10^{12}	194	1.8×10^{12}

times along y, and $N_z = N - N_y = N(2p-1)$ times along z. Then:

$$\tau_y = \frac{t}{N_y} = \frac{p}{2(1-p)}\tau_1 + \frac{1}{2}\tau_2 \tag{6}$$

$$\tau_z = \frac{t}{N_z} = \frac{p}{2p-1}\tau_1 + \frac{1-p}{2p-1}\tau_2 \tag{7}$$

The probability to be in a site 1 at jump n can be written as a function of the probability at jump $n-1$; it is the probability to be at a site 1 at jump $n-1$ multiplied by the probability to hop to a site 1, plus the probability to be at a site 2 at jump $n-1$ (as then it can only hop to a site 1):

$$p(n) = \left[p(n-1) \times \frac{k_{11}}{k_{11}+k_{12}} \right] + [1 - p(n-1)] \tag{8}$$

When stationnary, this leads to:

$$p = \frac{k_{11}+k_{12}}{k_{11}+2k_{12}} \tag{9}$$

Putting back Equations (9), (6), and (7) into Equation (3), we get:

$$D = D_2 = \frac{1}{3}\frac{k_{21}}{k_{12}+k_{21}}[l_z^2 k_{11} + 2l_y^2 k_{12}] \tag{10}$$

We are interested in what happens for a high energy barrier E_{12} and E_{21}. Let us write $\Delta E = E_{12} - E_{21}$, that is, ΔE represents the difference between the energies in sites 1 and 2; when $E_{12} \gg E_{11}$, D_2 has the limit value:

$$D_2(E_{12} \to \infty) \to \frac{v_{21}}{v_{12}\exp(\Delta E/kT) + v_{21}} D_1 \tag{11}$$

where:

$$D_1 = \frac{1}{3} l_z^2 k_{11} \tag{12}$$

is the diffusion coefficient that would be calculated if there was only one type of site. $D_2(E_{12} \to \infty)$ is strictly smaller than D_1, for any energy barrier E_{12}. This shows that

the existence of the second site influences the diffusion of the sorbed molecules: they indeed act as kinds of "molecular traps". Mathematically, this effect persists when the energy barrier $E_{12} \to \infty$, that is, when the probability to enter or leave a site 2 tends to zero: the residence time in the sites 2 indeed increases at the same rate as this probability decreases. However, the magnitude of the decrease of D_2 depends on the temperature of the system, and on the difference ΔE between the energies in the sites 1 and 2. Figure 6 shows a plot of D_2/D_1 in the case of 1-butene, calculated with Equations (10) and (12), as a function of the temperature for several values of the energy difference ΔE; the other parameters correspond to the values listed in Table 5; the distance between two adjacent sites is $l_y = 7.05$ Å and $l_z = 7.5$ Å. When $\Delta E = E_{12} - E_{21}$ is negative, site 2 is more stable than site 1; it is less stable when ΔE is positive. When $\Delta E = 0$, D_2 goes from the limit value $D_2(E_{12} \to \infty)$ at low temperature to the higher limit at very high temperature (it is not shown in the Figure, as it has no physical meaning: it is reached for temperatures above 10000 K). When ΔE is negative, then site 2 is a much better "trap" at low temperature, so that $D_2 \to 0$. On the contrary, when ΔE is positive, the sorbed molecule can more easily leave sites 2 than enter them, so that $D_2 \to D_1$. In the temperature range interesting for the adsorption of organics in zeolites, namely, 100–1000 K, D_2 stays clearly in the $D_2 < D_1$ regime, whatever ΔE.

The shape of this function suggests that this molecular trap effect happens for *any* energy barrier E_2 (provided that the second site is an energy minimum at least as stable as the first one). This is clearly not acceptable, as it would mean that the sorbed

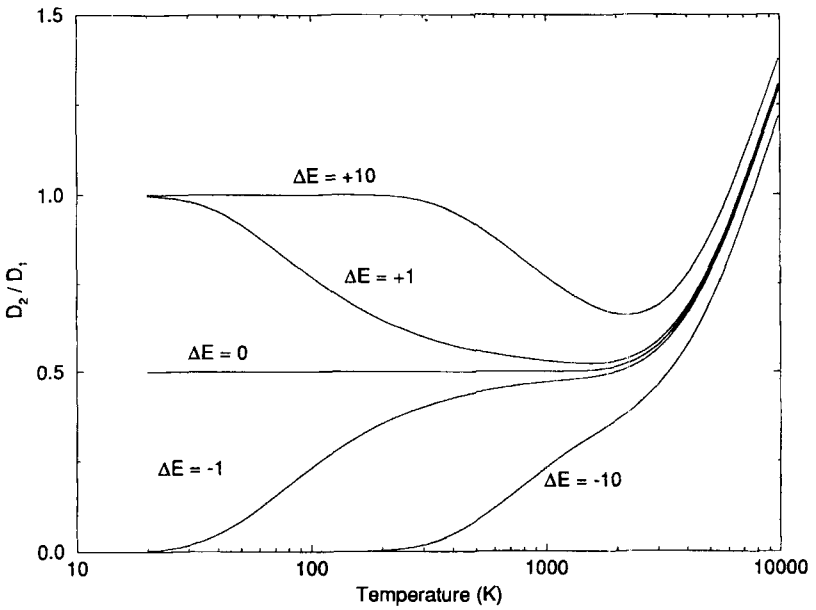

Figure 6 Evolution of D_2/D_1 with temperature, as determined by the analytical solution of the jump diffusion model (Eq. 10 and 12). Values of E_{ij} and v_{ij} are taken from Table 5 for 1-butene. Several $\Delta E = E_{12} - E_{21}$ (in kJ/mol) are considered for illustration.

molecule could enter a totally closed cavity. Therefore, when the energy barrier E_2 is high enough, the diffusion coefficient of the sorbed molecule should evolve according to D_1 (Equation (12)) rather than D_2 (Equation (10)), that is, the self-diffusion coefficient should *increase* when E_2 increases. We shall call the energy for which the diffusion coefficient of a given system changes from D_2 to D_1 the transition energy E_2^t, bearing in mind that this is no real transition, as the energy barrier for a real system is fixed. In the next Seciton, we determine this transition energy for butene isomers in ferrierite.

4.3 *Influence of the Experimental Conditions on the Diffusion Coefficient*

The transition from a "1 site" to a "2 sites" regime should take place when the energy barrier (at a given temperature) is too high for a molecule to be able to enter the sites 2 *during the time of an experience*, so that it does not follow the statistics described in the previous Section. This would only happen when E_{12} and $E_{21} \gg E_{11}$, so that the following simplifications can be adopted: the mean residence time of a molecule in the zeolite crystal becomes $t \approx N\tau_1$, where N is the mean number of jumps during t. The probability to find a molecule in a site 2 is then: $p' \approx k_{12}/k_{11}$. Writing the total number of molecules as $\mathcal{N}_{\text{mol}}$, the number of molecules that enter q times in a site 2 follows a Poisson law:

$$n(q) = \mathcal{N}_{\text{mol}} \frac{(Np')^q}{q!} \exp(-Np') \tag{13}$$

The global diffusion coefficient is:

$$D_2 = \frac{1}{\mathcal{N}_{\text{mol}}} \sum_q D(q)n(q) \tag{14}$$

A drastic approximation to $D_2(q)$ is the following: we consider that if a molecule cannot enter the site 2, its diffusion coefficient is D_1; if it enters one or more times, its diffusion coefficient is simply zero. Then D_2 can be approximated by:

$$D_2 \approx D_1 \exp(-Np') \tag{15}$$

For D_2 to be different from D_1 by less that 10%, it is sufficient that: $Np' < 1/10$, that is:

$$E_2 > E_2^t \approx kT \ln 20tv_{12} \tag{16}$$

We should note that the transition energy E_2^t depends on the mean residence time of the molecules in the zeolite, but not on the number of molecules. Furthermore, the dependence is logarithmic, so that even if the residence time becomes much longer, E_2^t remains in the same order of magnitude.

The mean residence time of the butene isomers in ferrierite during a catalytic experiment may be estimated from the experimental Weight Hourly Space Velocity (WHSV), which defines the rate with which the molecules are introduced into the reactor. Supposing that one unit cell of ferrierite may contain two butene molecules (the exact value is unimportant, as we are only interested in orders of magnitude), then

1 g of ferrierite saturated with butene contains 0.064 g of butene. Let x be the WHSV; in one hour, the zeolite is filled $x/0.064$ times, that is, the mean residence time (in seconds) can be written:

$$t = \frac{3600 \times 0.064}{x} \tag{17}$$

Experimental WHSV are typically 5–100 hour^{-1} [2, 3]. The mean residence time then is: $t \approx 2$–50 seconds. By using Equation (16) at 623 K, and with the values given on Table 5, we found the following transition energies $E_2^t \approx 165$–185 kJ/mol. Table 5 shows that the computed activation energies for the butene isomers leads to conclude that linear butenes, in the experimental conditions, would follow a 2 sites regime, while isobutene in the same conditions would follow a 1 site regime.

4.4 *Computed Diffusion Coefficient*

We have seen, considering good physical sense, that above a certain transition energy E_2^t, which depends on the experimental characteristics of the system, the diffusion coefficient of butene isomers in ferrierite undergoes a "transition" from a behavior described by sites 1 and 2 to one described by sites 1 only. Note again that this transition is not experimentally observable, as in real conditions the activation energy is fixed. Furthermore, it cannot be described by the analytical solution of the jump diffusion model, as it is due to the limited duration of the experiments. A computational representation of the behavior of the system should be able to reproduce this transition, as by definition it is performed over a limited number of steps. In the following Section, we give the details and results of such a model.

The following algorithm reproduces the behavior of the system. Its details are similar to the algorithm of Auerbach *et al.* [29]. We consider a single molecule in an infinite network of sites 1 and 2. At loop i, the molecule is initially in a site 1 or 2, at (x_i, y_i, z_i): at every loop, it hops to another site, and its coordinates are updated. If it was initially in a site 1, the time counter is increased by τ_1; if it was in a site 2, it is increased with τ_2. Coordinates (x_i, y_i, z_i) are recorded each time the time counter equals $n \times \tau_{bin}$, where n is an integer and τ_{bin} a reference time. If the time counter is incremented by a value larger than τ_{bin}, the same coordinates (x_i, y_i, z_i) are recorded several times in order for $n \times \tau_{bin}$ to reach the actual value of the time counter. This reference time insures an homogeneous time sampling, and avoids any difference due to the different scales of τ_1 and τ_2 when E_{21} and $E_{12} > E_{11}$.

The diffusion coefficient is readily calculated from the coordinates of the molecule, through Einstein's relation [20] (Equation (1)). In order to get better statistics, it is averaged over up to 2500 simulations for each point. We limited the length of the simulation to 50000 steps, which is equivalent to limit the simulated duration of the experiment to $t = N\tau_1$. As this simulated duration is much shorter than the real one, the corresponding transition energies are smaller than the one calculated in the preceding paragraph. The transition energy for each isomer becomes, according to Equation (16):

1-butene	trans-2-butene	cis-2-butene	isobutene
85 kJ/mol	71 kJ/mol	82 kJ/mol	96 kJ/mol

The evolution of the diffusion coefficients of all butene isomers in ferrierite, derived from the Jump Diffusion Model, is presented in Figure 7 as a function of the energy barrier E_{12}. The lines correspond to the diffusion coefficient D_2 calculated analytically by using Equation (10), while the points represent the diffusion coefficients computed by the JDM algorithm. We clearly see the similarity of the two solutions of the JDM for low energy barriers, as well as the transition which can only be observed on the computed diffusion coefficients. The transition energies agree well with the ones calculated by Equation (16), which shows that the transition criterium was well chosen.

This simple hopping model shows that the sites in the cavities along the 8-T channels, due to the high potential energy barrier the molecules have to overcome to

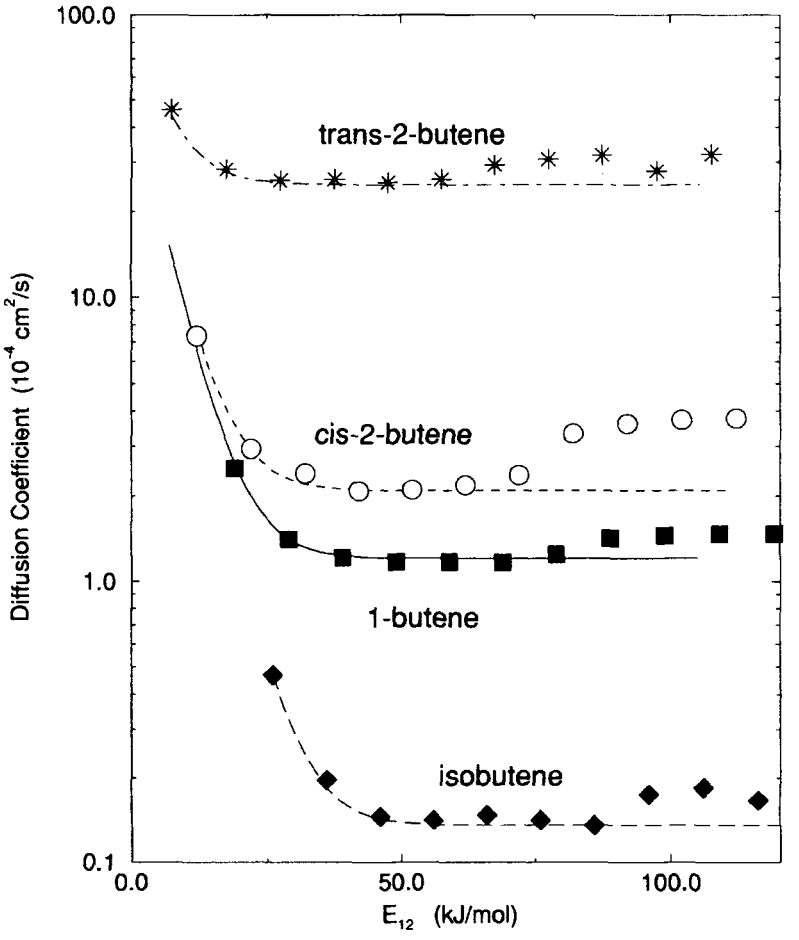

Figure 7 Evolution of the diffusion coefficients (D) of the butene isomers in ferrierite, as a function of the energy barrier E_{12} according to the jump diffusion model; symbols correspond to the computer simulation, total duration of 50000 steps, averaged over 250 simulations. The lines represent the diffusion coefficients from the analytic solution (Equation10).

enter or leave, act as molecular traps for linear butenes, thus slowing down their diffusion. On the other hand, the even higher potential energy barrier for isobutene prevents these molecules to be influenced by these sites, and their diffusion is not slowed down by this effect. As can be seen in Figure 7, taking this effect into account (in our simplified way) does not change the general ranking of the diffusion coefficient of the butene isomers: as for the molecular dynamics simulations, D(trans-2-butene) > D(1-butene) > D(cis-2-butene) > D(isobutene). We observe that the diffusional behavior of the butene molecules is mainly governed by the diffusion along the 10-T channels, which is not satisfactorily taken into account in an activated jump diffusion model.

5 DISCUSSION AND CONCLUSION

The study of Al substitution in a protonated ferrierite model with Si/Al = 8 has shown a preferential substitution on a T2 site, with the proton linked to a bridging oxygen at the intersection of the 8- and 10-T channels. The investigation of the energetics of the four butene isomers in this model of H-ferrierite gives several interesting results which allow to explain their diffusion properties.

More precisely, molecular docking has shown that the sorption energies of all butene isomers in ferrierite are within 6.3 kJ/mol of each other, isobutene being the less sorbed of all isomers. The same kind of argument was used by Freeman *et al.* to explain the selectivity of ZSM-5 toward isobutene [18]. In the case of ferrierite, one has to consider the energetics of butene isomers in two types of intersecting channels: in the 10-T channels, where isobutene is the less stabilized isomer, and in the cavities along the 8-T ring channels where trans-2-butene is the less sorbed molecule.

The diffusion of butene isomers in ferrierite cannot be completely understood *via* our molecular dynamics (MD) simulations: the supposed fixed framework and too short simulation runs (200 ps) prevent any accurate measurement of the diffusion time. However, the qualitative results obtained show a diffusion behavior consistent with the size of butene isomers: D(trans-2-butene) > D(1-butene) $\approx$ D(cis-2-butene) > D(isobutene). This behavior cannot explain the selectivity of ferrierite.

We nevertheless have shown, using a simple activated jump diffusion model, that the diffusion of the linear butenes in ferrierite is slowed down due to the influence of the cavities located in the 8-T channels, while these cavities do not influence the diffusion of isobutene. Therefore, the diffusion of isobutene should be enhanced relative to the other isomers in ferrierite, as compared with zeolite with similar 10-T channels but presenting no 8-T cavities, like ZSM-22 or ZSM-23; thus the presence of such cavities might be an important factor for the good selectivity of ferrierite. However, this slowing down does not change the order of magnitude of the self-diffusion coefficients; this shows that, around the temperature considered here (623 K), the self-diffusion behavior of the butene isomers in ferrierite is mainly due to the characteristics of their motions along the 10-T channels. Because of the low activation energy along this direction, these motions are not accurately taken into account in our simple model of activated jump diffusion. Moreover, as the size of isobutene is close to the size of the 10-T channels of ferrierite, neglecting the

vibrations of the zeolite in the MD study may introduce errors in the calculation of the diffusion coefficient. Derouane and coworkers indeed have predicted the existence of "floating molecules" in systems with restricted regions [33], which has been recently depicted by molecular dynamics simulations with flexible framework [34,35].

As the computed diffusion constant of trans-2-butene is very large, as compared with isobutene or the other linear isomers, trans-2-butene should be diffusing faster than all isomers. However, a study of Harrison *et al.* [8] of the bond isomerization of butene has shown that, at low conversion of 1-butene, cis-2-butene is the only reaction product in ferrierite. This indicates the existence, in the bond isomerization reaction, of a transition state selectivity, which adds to the shape selectivity of ferrierite. A similar transition state selectivity probably acts also in skeletal isomerization. The exact nature of the reaction mechanism has yet to be determined.

Acknowledgments

All authors wish to thank the FUNDP for the use of the Namur Scientific Computing Facility (SCF) Center. They acknowledge the financial support of the FNRS-FRFC, the "Loterie Nationale" for the convention no. 9.4593.92, the FNRS within the framework of the "Action d'impulsion à la recherche fondamentale" of the Belgian Ministry of Science under the convention no. D.4511.93., IBM Belgium for the Academic Joint Study on "Co-operative Processing for Theoretical Physics and Chemistry", and Biosym Technologies, Inc. for the use of their software in the framework of the "Catalysis and Sorption" consortium. F.J. acknowledges Prof. A. Lucas, Director of the PAI 3-49, and the European Union for the attribution of a post-doctoral fellowship in the framework of the HCM/Host Institution ERB CHBG CT930343 "Science of Interfacial and Mesoscopic Structures".

References

[1] J. Haggin, "Catalysts provide new route to isobutene", *C and E News*, **71** (31), 28 (1993).
[2] H. H. Mooiweer, K. P. de Jong, B. Kraushaar-Czarnetzki, W. H. J. Stork and C. C. H. Krutzen, "Skeletel isomerization of olefins with the zeolite ferrierite as catalyst", in *Zeolites and Related Microporous Materials: State of the Art 1994*, J. Weitkamp, H. G. Karge, H. Pfeifer and W. Hölderich eds, Elsevier, Amsterdam, 1994, pp. 2327–2334.
[3] W. -Q. Xu, Y. -G. Yin, S. L. Suib and C. -L. O'Young, "Coke formation and its effects on shape selective adsorptive and catalytic properties of ferrierite", *J. Phys. Chem.*, **99**, 758 (1995).
[4] W. -Q. Xu, Y. -G. Yin, S. L. Suib, J. C. Edwards and C. -L. O'Young, "n-butene skeletal isomerization to isobutylene on shape selective catalysts: ferrierite/ZSM-35", *J. Phys. Chem.*, **99**, 9443 (1995).
[5] P. A. Vaughan, "The crystal structure of the zeolite ferrierite", *Acta Cryst.*, **21**, 983 (1966).
[6] R. E. Morris, S. J. Weigel, N. J. Henson, L. M. Bull, M. T. Janicke, B. F. Chmelka and A. K. Cheetham, "A synchroton X-ray diffraction, neutron diffraction, ^{29}Si MAS-NMR, and computational study of the siliceous form of zeolite ferrierite", *J. Am. Chem. Soc.*, **116**, 11849 (1994).
[7] C. -L. O'Young, R. J. Pellet, D. G. Casey, J. R. Ugolini and R. A. Sawicki, "Skeletal isomerization of 1-butene on 10-membered ring zeolite catalysts", *J. Catalysis*, **151**, 467 (1995).
[8] I. D. Harrison, H. F. Leach and D. A. Whan, "Comparison of the shape selective properties of ferrierite, ZSM-5, and ZSM-11", *Zeolites*, **7**, 21 (1987).
[9] M. W. Simon, S. L. Suib, and C. -L. O'Young, "Synthesis and characterization of ZSM-22 zeolites and their catalytic behavior in 1-butene isomerization reactions", *J. Catalysis*, **147**, 484 (1994).

[10] S.Natarajan, P. A. Wright and J. M. Thomas, "Catalytic isomerisation of but-1-ene to 2-methylpropene over solid acids: comparison between DAF-1 and other shape selective magnesium-containing aluminophosphates and aluminosilicates", *J. Chem. Soc., Chem. Commun.*, 1861 (1993); R. G. Bell, D. W. Lewis, P. Voigt, C. M. Freeman, J. M. Thomas and C. R. A. Catlow, "Computer modelling of sorbates and templates in microporous materials", in *Zeolites and Related Microporous Materials: State of the Art 1994*, J. Weitkamp, H. G. Karge, H. Pfeifer and W. Hölderich eds, Elsevier, Amsterdam, 1994, pp. 2075–2082.

[11] J. G. Fripiat, P. Galet, J. Delhalle, J.-M. André, J. B'Nagy and E. G. Derouane, "A non-empirical molecular orbital study of the siting and pairing of aluminum in ferrierite", *J. Phys. Chem.*, **89**, 1937 (1985).

[12] K. P. Schröder, J. Sauer, M. Leslie and C. R. A. Catlow, "Siting of Al and bridging hydroxyl group in ZSM – 5: a computer simulation study", *Zeolites*, **12**, 20 (1992).

[13] *Discover User Guide*, version 94.0 Biosym Technologies, San Diego, 1994.

[14] J.-R. Hill and J. Sauer, "Molecular mechanics potential for silica and zeolite catalysts based on ab initio calculations. 1. Silicates", *J. Phys. Chem.*, **98**, 1238 (1994); id., "2. Aluminosilicates", *ibid.*, **99**, 9536 (1995).

[15] M. -H. Fêng and K. -J. Chao, "A theoretical study of aluminium substitution in MFI zeolites", *J. Chin. Chem. Soc.*, **41**, 679 (1994).

[16] See, *e. g.*, K. S. Smirnov, "Computer simulation study of methane in silicalite", *Chem. Phys. Letters*, **229**, 250 (1994); J. B. Nicholas, F. R. Trouw, J. E. Mertz, L E. Iton and A. J. Hopfinger, 'Molecular dynamics simulation of propane and methane in silicate", *J. Phys. Chem.*, **97**, 4149 (1993); M. Ghosh, G. Ananthakrishna, S. Yashonath, P. Demontis and G. Suffritti, "Probing potential energy surfaces in confined systems: behavior of mean-square displacement in zeolites", *J. Phys. Chem.*, **98**, 9354 (1994); and references therein.

[17] H. Papp, W. Hinsen, M. T. Do and M. Baerns, "The adsorption of methane on H-ZSM-5 zeolite", *Thermochim. Acta*, **82**, 137 (1984); A. S. Chiang, A. G. Dixon, Y. H. Ma, "The determination of zeolite crystal diffusivity by gas chromatography 2. Experimental", *Chem. Eng. Sci.*, **39**, 1461 (1984).

[18] C. M. Freeman, C. R. A. Catlow, J. M. Thomas and S. Brode, "The location and energetics of organic molecules in microporous adsorbents and catalysts: a hybrid approach applied to isomeric butenes in a model zeolite", *Chem. Phys. Letters*, **186**, 137 (1991).

[19] See, *e.g.*, L. Leherte, J.-M. André, E. G. Derouane and D. P. Vercauteren,, "What does zeolitic water look like?: modelization by molecular dynamics simulations", *Int. J. Quant. Chem.*, **42**, 1291 (1992); and references therein.

[20] M. P. Allen and D. J. Tildesley, *Computer Simulations of Liquids*, Clarendon Press, Oxford, 1987.

[21] E. J. Maginn, A. T. Bell and D. N. Theodorou, "Low-occupancy sorption thermodynamics of long alkanes in silicalite via molecular simulation", in *Zeolites and Related Microporous Materials: State of the Art 1994*, J. Weitkamp, H. G. Karge, H. Pfeifer and W. Hölderich eds, Elsevier, Amsterdam, 1994, pp. 2099 – 2105.

[22] B. Smit and J. Ilja Siepmann, "Simulating the adsorption of alkanes in zeolites", *Science*, **264**, 1118 (1994).

[23] R. L. June, A. T. Bell and D. N. Theodorou, "Molecular dynamics studies of butane and hexane in silicalite", *J. Phys. Chem.*, **96**, 1051 (1992).

[24] E. Hernández and C. R. A. Catlow, "Molecular dynamics simulations of *n*-butane and *n*-hexane diffusion in silicalite", *Proc. Roy. Soc. Lond. A*, **448**, 143 (1995).

[25] N. J. Henson, A. K. Cheetham, B. K. Peterson, S. D. Pickett and J. M. Thomas, "An investigation of transport and sorption properties of xenon in ferrierite and zeolite L using molecular dynamics", *J. Comput.-Aided Mat. Design*, **1**, 41 (1993).

[26] J. Caro, M. Bülow, W. Schirmer, J. Kärger, W. Heink, H. Pfeifer and S. P. Zdanov, "Microdynamics of methane, ethane and propane in ZSM-5 type zeolites", *J. Chem. Soc. Faraday Trans. I*, **81**, 2541 (1985).

[27] D. Theodorou and J. Wei, "Diffusion and reaction in blocked and high occupancy zeolite catalysts", *J. Catalysis*, **83**, 205 (1983).

[28] R. M. Barrer and L. V. C. Rees, "Sorption and mixtures, part 3. Polar sorbates as modifiers of zeolite crystals", *Trans. Faraday Soc.*, **50**, 989 (1954).

[29] S. M. Auerbach, N. J. Henson, A. K. Cheetham and H. L. Metiu, "Transport theory for cationic zeolites: diffusions of benzene in Na-X". *J. Phys. Chem.*, **99**, 10600 (1995).

[30] R. L. June, A. T. Bell, and D. N. Theodorou, "Transition state studies of xenon and SF_6 diffusion in silicalite", *J. Phys. Chem.*, **95**, 8866 (1991).

[31] A. F. Voter and J. D. Doll, "Dynamical corrections to transition state theory for multistate systems: surface self-diffusion in the rare event regime", *J. Chem. Phys.*, **82**, 80 (1985).

[32] P. W. Atkins, *Physical Chemistry*, fifth edition, Oxford University Press (1994).
[33] E. G. Derouane, J.-M. Andrè and A. A. Lucas, "Surface curvature effects in physisorption and catalysis by microporous solids and molecular sieves", *J. Catalysis*, **110**, 58 (1988); I. Derycke, J.-P. Vigneron, Ph. Lambin, A. A. Lucas and E. G. Derouane, "Physisorption in confined geometry", *J. Chem. Phys.*, **94**, 4620 (1991).
[34] P. Santikary and S. Yashonath, "Dynamics of zeolite cage and its effect on the diffusion properties of sorbates: persistence of diffusion anomaly in NaA zeolite", *J. Phys. Chem.*, **98**, 9252 (1994).
[35] S. Yashonath and S. Bandyopadhyay, "Surprising diffusion behavior in the restricted regions of silicalite", *Chem. Phys. Lett.*, **228**, 284 (1994).